Ocean Science Journal, Vol. 42 No. 1, 19-30(2007)

Article

Ocean Science Journal

http://osj.kordi.re.kr

Tidal and Sub-tidal Current Characteristics in the Kangjin Bay, South Sea, Korea

Young Jae Ro

Department of Oceanography, College of Natural Sciences, Chungnam National University, Daejon 305-764, Korea

Received 22 February 2006; Revised 14 March 2007; Accepted 15 March 2007

Abstract – This study analyzed the current meter records along with wind records for over 500 days obtained in the Kangjin Bay, South Sea, Korea spanning from March, 2003 to Nov. 2005. Various analyses include descriptive statistics, harmonic analysis of tidal constituents, spectra and coherence, the principal axis, progressive vector diagrams. These analyses can illustrate the response of residual current to the local wind resulting in the net drift with rotational motion. Current speed ranges from -28 to 33 (cm/sec), with standard deviations from 6.5 to 12.9 (cm/sec). The harmonic analyses of the tidal current show the average form number, 0.12 with semi-diurnal type and the recti-linear orientation of the major axis toward northeast. The magnitudes of the semi-major range from 12.7 to 17.7 (cm/sec) for M2 harmonics, while for S2 harmonics, they range from 6.3 to 10.4 (cm/sec), respectively. In the spectral and coherency analysis of residual current and wind, a periodicity of 13.6 (day) is found to be most important in both records and plays an important role in the net drift of residual current. The progressive vector diagrams of residual current and wind show two types of behaviors such as unidirectional drift and rotational motion. It was also found that 3 % rule holds approximately to drive 1 (cm/sec) drift current by 30 (cm/sec) wind speed based on the correlation of the semi-major axis of wind and residual current.

Key words – current, tidal harmonics, spectra, principal axis, progressive vector

1. Introduction

Intensive field measurements and realtime monitoring of the hydrographic, current and meteorological conditions in the Kangjin Bay, South Sea were carried out for the period of Sept., 2003 to Aug., 2006 and have produced an unprecedented amount of datasets for this study. Detailed report can be referred to Ro (2006). Among those, current meter and Automatic Weather System records of over 508 days are subject to various analyses to find out the tidal and residual current characteristics in terms of basic statistics, harmonic analysis, spectral characteristics, principal axis of residual current, and wind. The database provides a rare opportunity to characterize dynamical characteristics as well as wind and tide variations' impact on the local fishery and ecosystem dynamics, particularly for the large-arc shell (*Scapharca Broughtonii*).

Previous studies for the tidal current and its residual current in the Kangjin Bay (hereafter KB) have not been carried out yet to the author's knowledge. However, several studies are noteworthy for the relevant information in the neighboring water bodies such as Chang *et al.* (1993) and Cho *et al.* (2002) for the circulation and stratification condition and DO concentration in the Jinhae Bay, Cho *et al.* (1993) for the circulation and material flux in the Deuk Ryang Bay. Lee *et al.* (2006) investigated the current measurements to investigate the tidal characteristics as well as long-term residual current in the Kwang Yang Bay in which Lee *et al.* (2005) and Park *et al.* (2005) made numerical modeling of the water quality.

Numerous studies have been made to investigate the tidal residual currents in the coastal and estuarine environments throughout the world. Among those, some are most relevant to this study. Ou *et al.* (1980) analyzed the subtidal current fluctuations in the Middle Atlantic Bight using spectral and coherence estimates. Yasuda (1980) and Yanagi (1983) investigated the residual currents in the Tokyo Bay in the

*Corresponding author. E-mail: royoungj@cnu.ac.kr

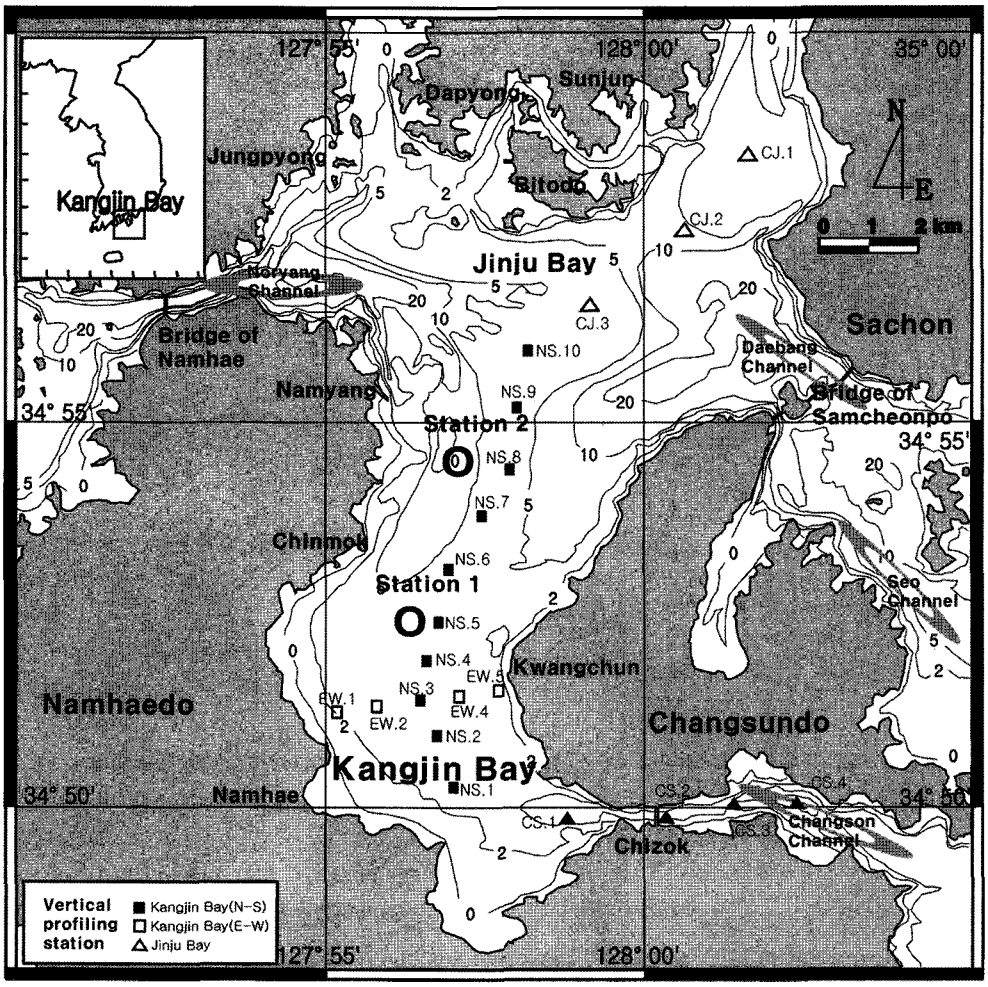

Fig. 1. The Kangjin Bay in the South Sea with bottom topography. Current meter mooring and meteorological AWS at Station 1.

early 80's. Liu (1992) investigated the influence of episodic weather events on tidal residual currents in the Sebastian Inlet, Florida. Many investigators carried out numerical modelings to understand the mechanism for the generation of the residual current (Kashiwai 1984; Guo and Yanagi 1996; Cai *et al.* 2003; Marinone and Lavin 2005; Foreman *et al.* 2006). Low frequency and subtidal characteristics in the Delaware coastal current was investigated by Wong (1998) in that spectral and coherency characteristics were examined. Valle-Levinson and Matsuno (2003) investigated the tidal and subtidal flow in the East China Sea.

The objectives of this study are as follows;

1) characteristics of tidal current in terms of tidal ellipse parameters in Section 3,

2) spectral and coherency characteristics of residual current and wind in Section 4,

3) principal axes of the residual current and the influence of local wind on the net drift of the residual current in Section 4.

2. Material and Method

In carrying out the KB Project (Ro 2006), intensive field work had been carried out to collect the hydrographic and hydrodynamic conditions such as water temperature and salinity, current speed and direction; meteorological parameters such as wind speed and direction, solar irradiance and humidity, *etc.* The current meter records produced from March, 2003 to July, 2006 amount to 508 day-worth data by using Aanderraa Current Meter (RCM 9). Among those, current records of periods over 17 days without interruptions and malfunctioning are chosen for detailed analysis in this study. These long-term current records

Table 1. Specifications for the tidal record collected in the Kangjin Bay during year 2004-2005.

Record #	Start date	End date	Length (days)
1	2004-03-22	2004-04-11	20.6
2	2004-04-16	2004-09-22	158.8
3	2004-11-09	2005-04-11	153.5
4	2005-04-24	2005-08-14	112.0
5	2005-09-03	2005-11-06	63.96

over more than five months without interruption in the coastal waters provide a very rare opportunity to investigate the various characteristics of coastal currents in terms of tidal and non-tidal dynamics. During the periods of current meter records, records of wind speed and direction were simultaneously obtained *in situ* by using Aanderraa AWS at the height of 9 (m) above sea level (Fig. 1).

The details of the current measurement records in the KB are summarized in Table 1. For the analysis of the current records, data quality check was pre-processed to eliminate any possible noises by conventional statistical screening method. Velocity decomposition is made in terms of north-south (v) component and east-west (u) component and then each record are subject to various analyses. Fig. 2 show the time series of current records listed in Table 1 where, in general, the semi-diurnal tidal oscillation modulated by neap-spring tidal cycle is obvious and other non-tidal and sub-tidal components are inherent.

To investigate the characteristics of coastal current, several analysis methods were adopted in that 1) Current meter records were subject to harmonic analysis to estimate tidal constituents and tidal ellipse parameters were estimated

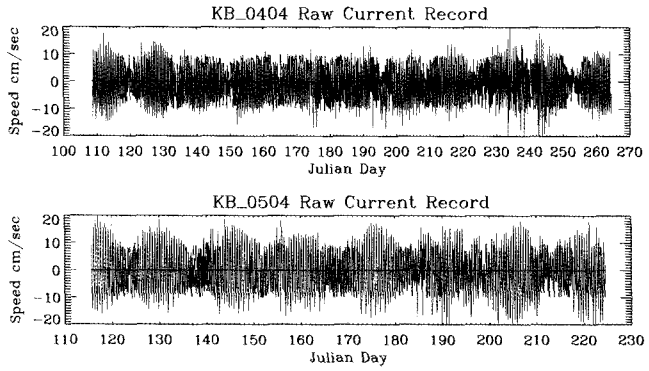

Fig. 2. Time series of the raw current meter records in the Kangjin Bay for the Record #2, 4. Blue(black) line represents v(u)-component of the velocity.

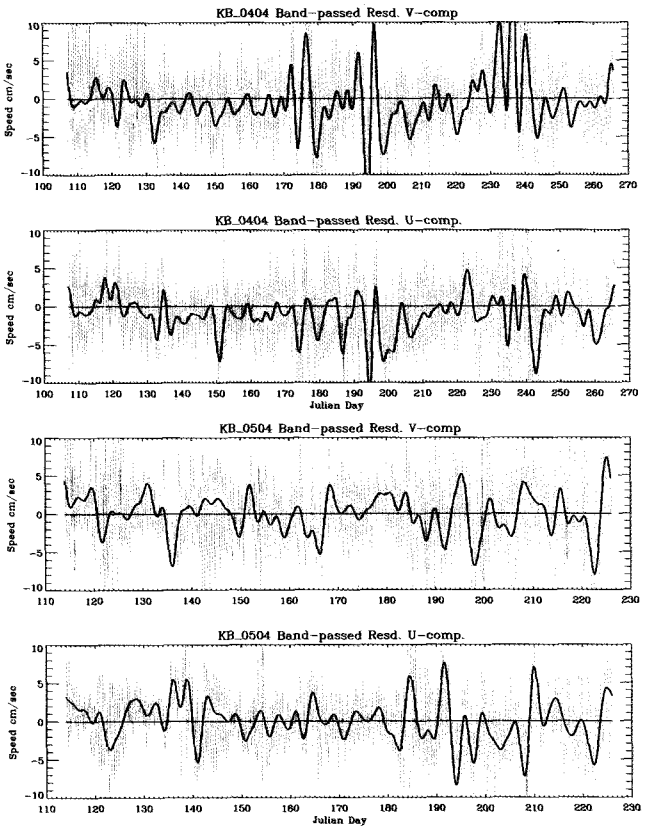

Fig. 3. Time series of the residual current in the Kangjin Bay for the Record #2, 4, shown in yellow color. Thick black lines represent band-passed residual current speed multiplied by a factor of 2.

based on the classical technique (Foreman 1978) and Matlab program package provided by Pawlowicz *et al.* (2002) was useful. In Section 3, the results of harmonics analysis will be described, 2) after detiding the current records by subtracting the tidal harmonics estimated, residual current records (Fig. 3) were prepared for further analyses in which 3) spectral and coherence characteristics, 4) principal component axis (hereafter, pca) of current and wind, 5) progressive vector diagram were investigated. Spectral and coherency analyses were carried out by using classical methods based on FFT algorithm by Blackman and Tukey (1958) and Jenkins and Watts (1968). Smoothing was applied to the tidal residual current by using Lanczos band-pass filters with cutoff periods of 3 and 30 days. Number of weights used in filtering exceeds 211 data points which correspond to 7-day worth data to insure satisfactory response function of weights used (Duchon 1979). The smoothing would help to understand the behavior of residual drift current with rotational motion in association

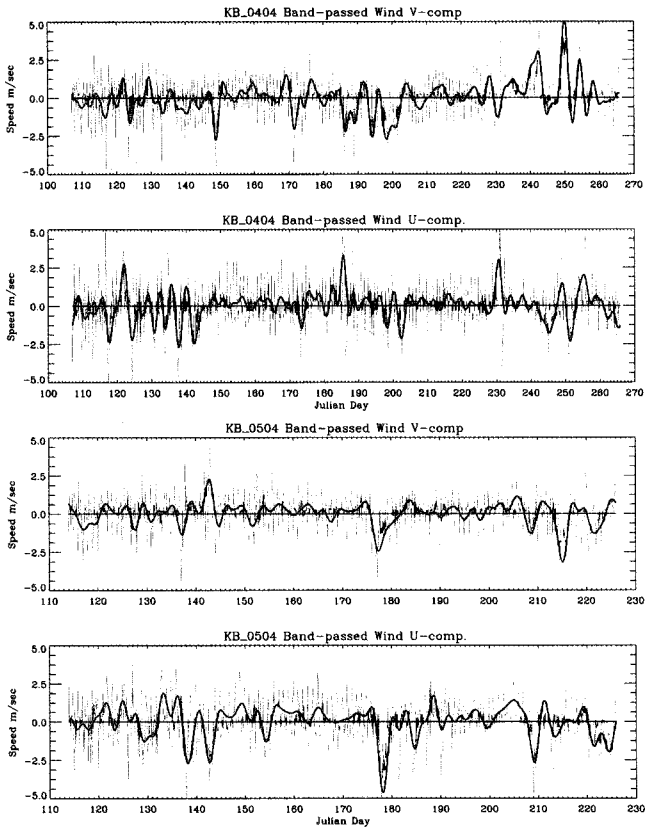

Fig. 4. Time series of the corresponding wind records in the Kangjin Bay. Thick black lines represent band-passed wind speed multiplied by a factor of 2.

with wind. Confidence interval for the coherency estimates were referred to Wang and Tang (2004). Section 4 will show the sub-tidal oscillation of coastal current and will be described and analyzed in terms of the spectral and coherence characteristics with wind shown in Fig. 4. The method of pca was referred to Emery and Thomson (2001) which is applied to both the residual current and wind vector time series to yield major axis along which variance of fluctuation is maximized. Those results are described in Section 4.

3. Characteristics of Tidal Current

Descriptive statistics of current record

To understand the basic characteristics of the current behaviors, descriptive statistics are presented in Table 2. The estimated statistics are based on mean, standard deviation, mini- and maximal values of current components. Mean velocity components show ranges of 0.05 to 1.3 (cm/sec) for u-comp. and 0.09 to 0.35 (cm/sec) for v-comp. indicating the net drifts to certain directions during each period. Standard deviations (hereafter st. dev.) range from 6.5 to 8.5 (cm/sec) for u-comp., and 9.5 to 12.9 (cm/sec) for v-components. The mean and st. dev. for each component indicate the existence of asymmetry between current components. Mean values are attributed to the net drift, while st. dev. represents the variability of the component velocity. In the KB, stronger variability exists for v-comp. than u-comp., since the size of the physical geometry is bigger in the north-south direction than in the east-west one. Net drifts of the currents are related to sub-tidal fluctuation, which will be analyzed and discussed by means of progressive vector diagram in the following Section 4.2.

Maximal velocity values of eastward and northward velocity components show 33.49 and 33.23 while the westward and southward velocity components show 26.56 and 28.85 (cm/sec), respectively. However, it is noteworthy that the current speeds may exceed higher than 4 knots in the other locations such as Noryang, Changson and Daebang Channels at maximal tidal phases.

Harmonic analysis of tidal current

To further understand the characteristics of the tidal current in the KB, the records were analyzed in terms of tidal harmonics. Number of tidal constituents in the least fitting estimation of the tidal harmonics is limited by each record length in Table 1. Since the Record #1 is only 20

Table 2. Statistics of current records in terms of mean, standard deviation, mini- and maximal values of u- and v-components.

Record #	u-comp (cm/sec)				v-comp (cm/sec)			
	mean	st. dev.	mini	maxi	mean	st. dev.	mini	maxi
1	-0.36	7.81	-17.22	15.54	0.22	12.91	-26.99	32.20
2	-1.05	6.51	-26.56	20.70	-0.54	9.51	-27.01	27.31
3	-0.77	8.23	-20.52	33.49	0.35	12.10	-28.85	33.23
4	-0.05	8.53	-22.51	19.58	-0.09	11.77	-27.64	28.76
5	-1.30	8.06	-20.72	18.47	0.18	11.52	-24.91	29.53

Table 3. The results of the harmonic analyses for the current meter records. Acronyms of Var and % Var are used for total variance of records and percentage of variance explained by 4 major tidal constituents. Notions of sma, smi, inc and pha stand for the semi-major, semi-minor axes and angle of the inclination in deg. and phase lag for the tidal ellipse parameters. (-) sign for smi indicates counter-clockwise rotation of tidal ellipse. Units for tidal constituents are (cm/sec).

Record #	Const.	sma	smi	inc	pha	U-comp.		V-comp.	
						Var	%Var	Var	%Var
1	O1	0.95	-0.12	44.76	267.13	57.1	93.4%	157.5	94.3%
	K1	0.67	-0.06	38.56	276.32				
	M2	16.49	0.94	59.13	1.51				
	S2	10.39	0.51	58.69	41.32				
2	O1	0.65	-0.16	42.45	20.70	28.9	69.0%	76.5	81.3%
	K1	2.13	-0.40	54.42	41.33				
	M2	12.69	0.94	59.30	243.62				
	S2	6.29	0.21	56.48	258.12				
3	O1	1.04	-0.04	51.64	97.12	61.1	89.8%	137.3	93.3%
	K1	1.81	0.11	48.61	124.75				
	M2	17.19	0.34	56.06	29.11				
	S2	8.47	0.31	57.13	56.25				
4	O1	1.36	0.00	40.05	61.31	60.9	83.6%	124.6	89.1%
	K1	2.19	-0.03	56.48	63.41				
	M2	17.65	0.22	55.30	317.51				
	S2	6.50	0.08	53.73	339.22				
5	O1	1.16	-0.08	39.04	52.02	60.2	92.0%	125.9	94.2%
	K1	1.62	-0.13	52.63	60.45				
	M2	15.74	-0.07	55.28	287.03				
	S2	9.71	0.12	55.67	293.25				

days long, the resolvable number of harmonics is limited to 17 constituents with Msf, longest harmonic of 0.0028219 (cph). The other 4 records could yield estimates of 35 tidal constituents with Mm 0.0015122 (cph).

Table 3 shows only the four major harmonics of M2, S2, K1 and O1 among others with semi-major and minor, inclination angle and phase lag relative to the Greenwich. Also given are the variance of velocity components and percentage contribution of the tidal harmonics to total variance. As a summary, the results of the harmonic analyses show that semi-major and -minor axes range from 12.69 to 17.65 (cm/sec) and 0.07 to 0.94 (cm/sec) for M2 constituent, while for S2 constituent, they range from 6.3 to 10.4 (cm/sec) and 0.08 to 0.51 (cm/sec), respectively. Average ratio of S2 to M2 semi-major axis is 0.53, indicating that M2 tidal components are about twice as big as S2 components. For diurnal components, semi-major and -minor axes range from 0.67 to 2.19 (cm/sec) and 0.03 to 0.4 (cm/sec) for K1 harmonics, while for O1 harmonics, they range from 0.01 to 1.16 (cm/sec) and 0.0 to 0.16 (cm/sec), respectively. Average ratio of O1 to K1 semi-major axis is 0.45 indicating that K1 tidal components are about 2.2 times bigger than O1 components. The average form number for these 5 records is 0.12 indicating that the tidal current is very much of semi-diurnal type. The ratio of semi-minor axes to semi-major axes of 4 major constituents ranges from 0.05 to 0.89 with average of 0.31, indicating that the tidal current in the KB is strongly rectilinear. The mean ratio of semi-minor axes to semi-major axes of M2, S2, K1, O1 are 0.03, 0.03, 0.09, and 0.10 respectively. The mean inclination angles of M2, S2, K1, O1 are 57, 56, 50, and 44 (deg.), respectively indicating that major tidal current is oriented toward northeast-southwest. However, as seen in Table 3, the tidal current records exhibit strong seasonal and inter-annual variation.

The contributions of tidal harmonics to the total variances of current fluctuation vary among current records in different time periods. In Table 3, contributions of tidal harmonics to total variances account for over 90 % in most records except the Record #2 with lowest 69 % for the u-component. This fact implies the role of non-tidal dynamics. In particular, the low percentage accounting of

Table 4. Basic statistics of band-passed residual current.

Record #	U-comp				V-comp			
	Mean	Std. Dev.	Min	Max	Mean	Std. Dev.	Min	Max
2	-0.70	1.22	-5.06	2.37	-0.35	1.57	-7.09	5.79
3	-0.52	0.72	-3.57	1.68	0.24	0.46	-0.87	2.12
4	-0.04	1.35	-4.49	3.94	-0.03	1.24	-3.88	3.35
5	-0.84	0.76	-2.60	1.48	0.14	0.66	-1.50	2.50

tidal harmonics for total variance is attributed to the density current produced by the Nam-Gang Dam water discharge during the Typhoon 'Megi' passage in the middle of August, 2004. These will be discussed in the Section 4.3.

The residual current records prepared in Section 2 are analyzed to show the basic statistics in Table 4. Maximal values of eastward and northward residual velocity components show 3.94 and 5.79 while the westward and southward velocity components show 5.06 and 7.09 (cm/sec), respectively. The asymmetry between north- and south-ward and east- and west-ward velocity components resulted in the south-westward net drift in the KB at the current meter station. This will be more exploited in Section 4.2.

4. Sub-tidal Current Characteristic

Spectral characteristics of residual current

Fig. 5 shows the spectra of the band-passed residual current components of u and v for the Records #2, 3 and 4. Table 5 lists the periods of significant spectral peaks

Table 5. Percentage contribution to total variance of residual current by the significant spectral peaks.

Record #	resd_u		resd_v	
	Period (day)	%	Period (day)	%
2	12.9	1.7	11.1	1.6
	8.7	2.7	7.8	1.8
	4.6	0.4	4.6	1.1
3	6.0	1.7	11.6	3.9
	4.0	0.9	8.7	1.5
			4.4	0.3
4	13.6	5.1	13.6	9.6
	6.4	2.9	6.4	1.5
	4.7	1.0	4.5	0.6

for the residual current and smoothed wind. These peak periods represent various periodicities ranging from 3.6 to 36.3 days. The largest amplitudes of residual current at the frequency of 0.019 (cpd) are 0.70 (cm/s) and 0.54 (cm/s) for north and east components for the Record #2, at the frequencies of 0.013, 0.169 (cpd), 0.24 (cm/s) and 0.26 (cm/s) for north and east components for the Record #3, at the frequencies of 0.125, 0.268 (cpd), 0.60 (cm/s) and 0.56

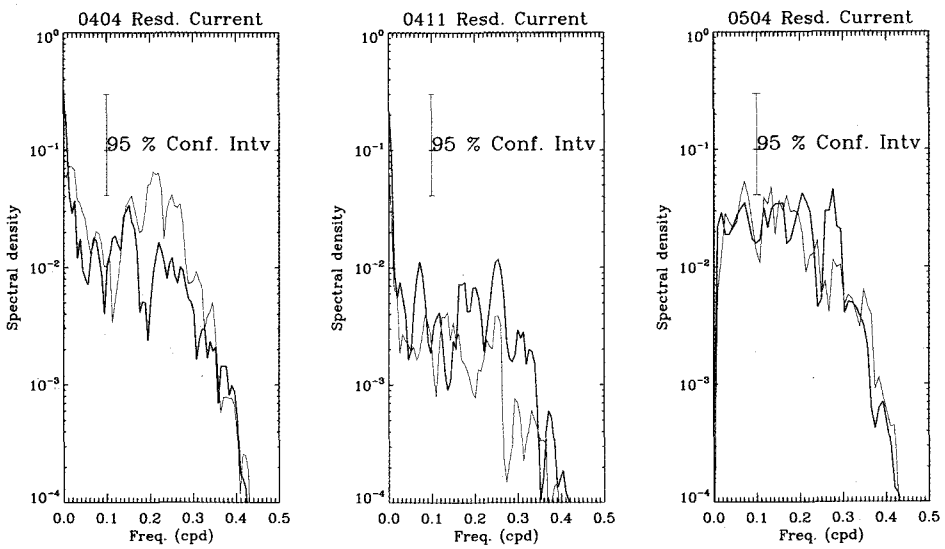

Fig. 5. Spectra of the band-passed time series of the current meter records, 0404, 0411, 0504. Red (black) line represents v(u)-comp. of current records.

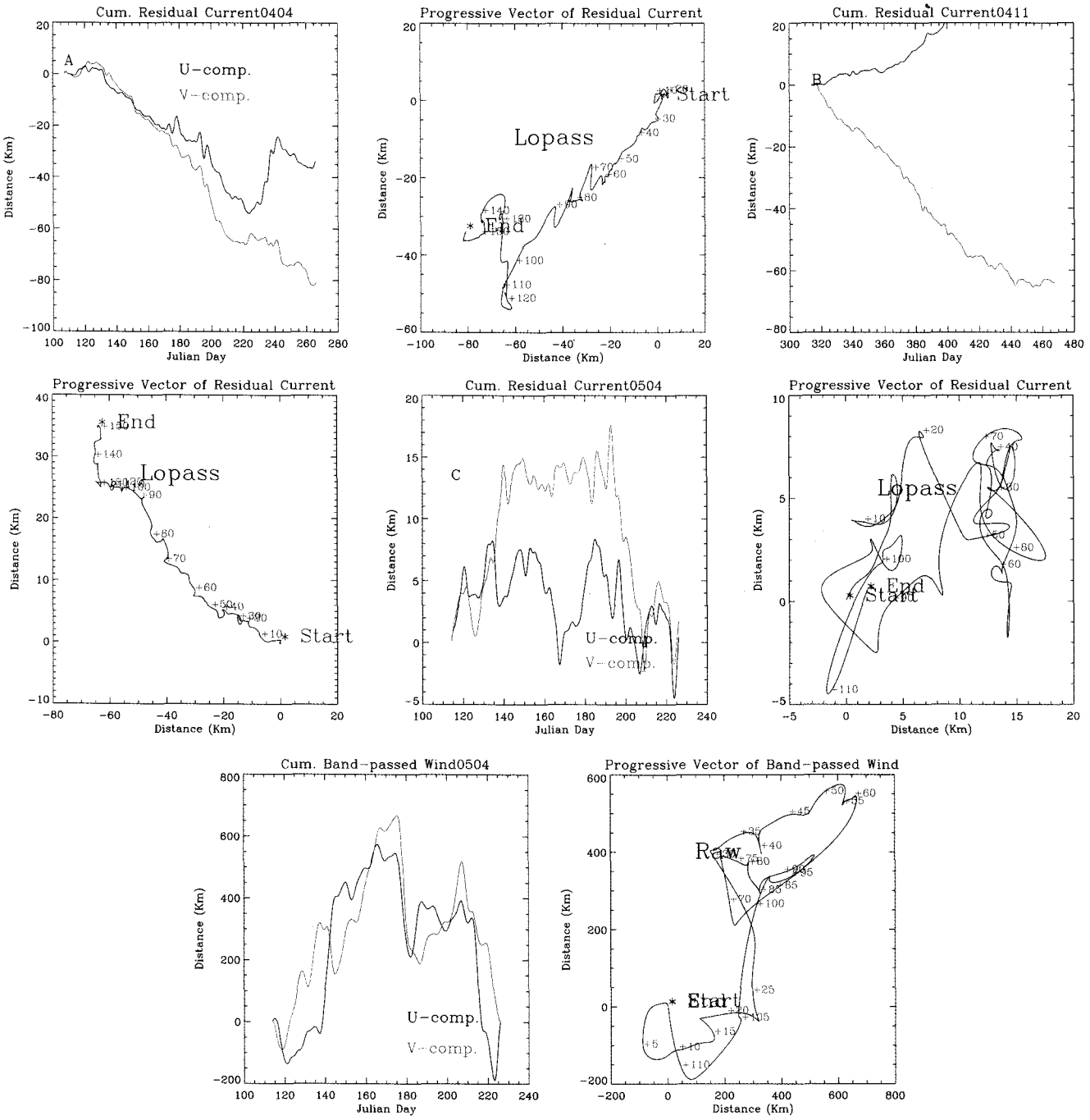

Fig. 6. Progressive vector diagrams for band-passed residual current (Record # 2, 3, and 4). Left panel shows the cumulative travel distances by each component of current. In Fig. 6c, pvd of wind is compared to that of residual current. Red(black) line represent the v(u)-comp. of wind and current.

(cm/s) for north and east components for the Record #4, respectively. In general, they can be summarized into the period bands of month, half month, week and 4 days. These frequencies lie closely on the folding frequencies of 1/30 (cpd).

The degree of contributions of low frequency components to total variances in the band-passed time series vary from record to record. Table 5 is prepared to show the relative contribution to total variances made by the significant spectral peaks listed in Table 5. In most of the cases, the percentage scores of relative contribution to total variance made by single frequency component are less than 5 %.

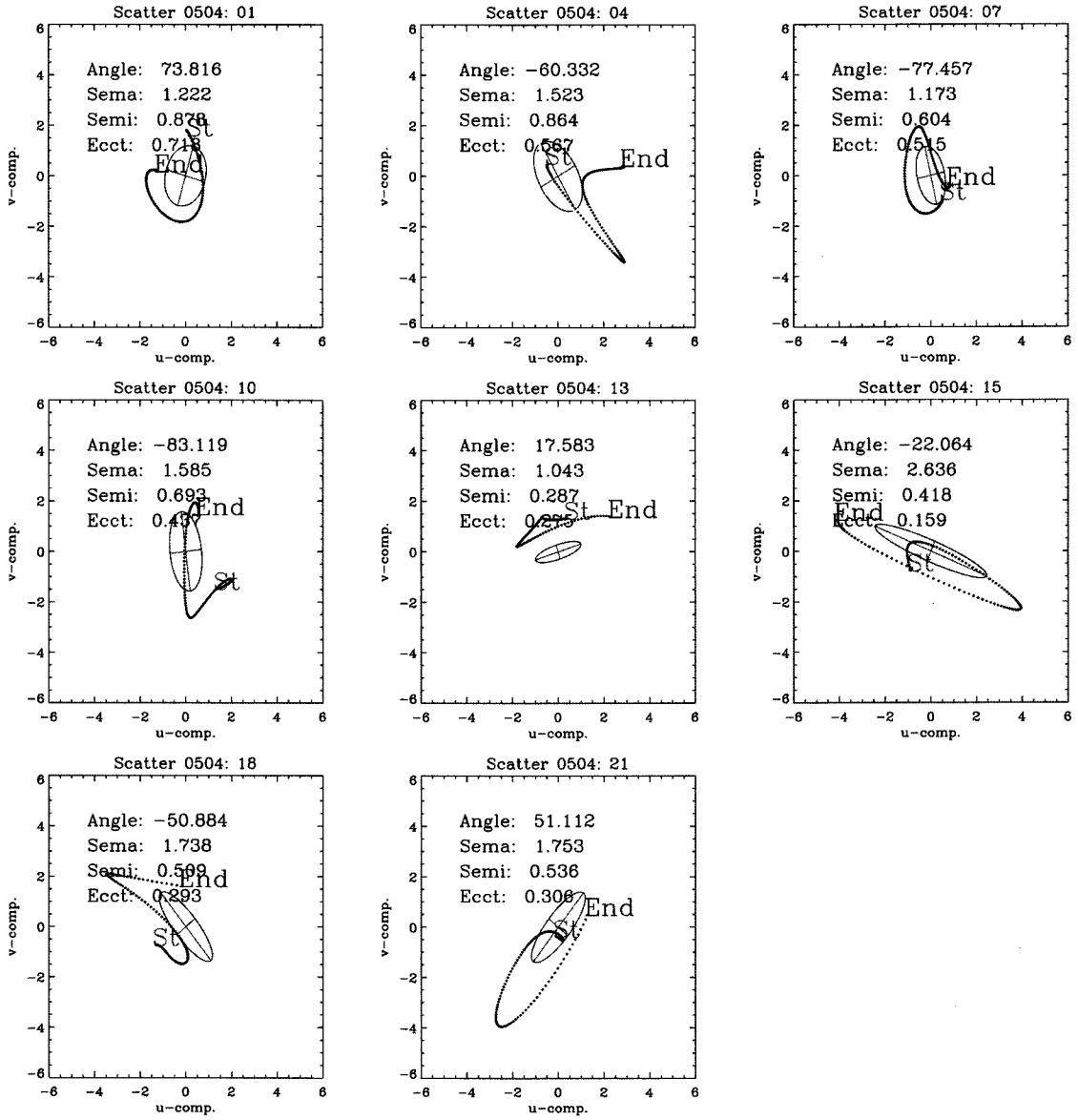

Fig. 7. Time sequence of ellipses with scatter diagram of residual current for the Record #4.

Two exceptions are notable for the Record of #4. Spectral components of 13.6-day period represent 5.1 % and 9.6 % of the total variances of the velocity components for the Record #4, respectively.

Influence of the local wind on the residual current

In the KB, the influence of the local wind on the residual current is important, yet very complicated due to many factors such as local complex coastline geometry, bottom topography, open boundaries, etc. However, its influence is investigated in terms of two domains, namely, time and frequency. In time domain, behaviors of progressive vectors for each residual current record are investigated in terms of cumulative travel distances. In frequency domain, spectral characteristics in term of cross-spectra and coherency between residual current and wind are analyzed.

First, the behavior of the residual current could be understood in terms of progressive vector diagrams shown in Fig. 6. Two types of behaviors are obvious: that in Type I, unidirectional drift is apparent in a particular direction in the Records of #2 and 3, while in Type II, rotational motion is more influential during the course of drift so that the trajectories look more complicated and wiggle in the Records #4.

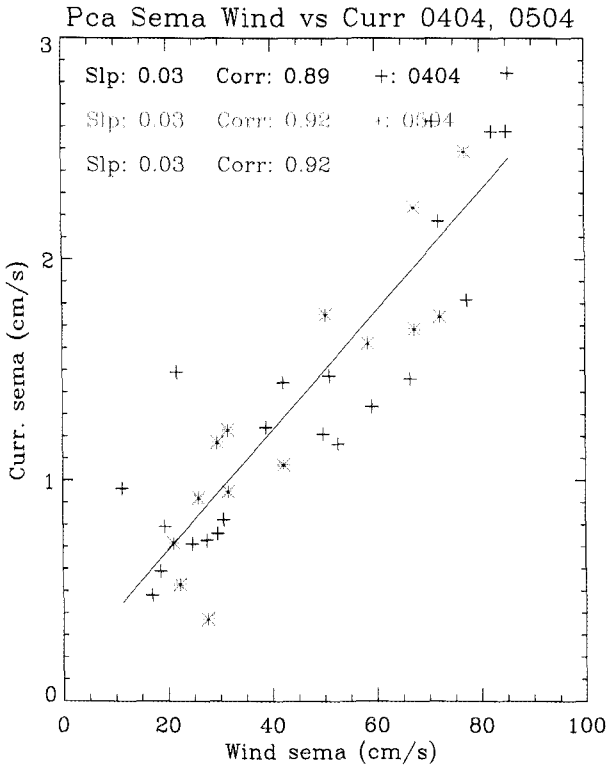

Fig. 8. Correlation between the semi-major axis of wind versus residual current for the Records #2 and 4.

Among those, Record #4 deserves further investigation to explain the complicated and somewhat interesting aspect of trajectories. In Fig. 6c, the cumulative drift of residual current shows 7 local maxima and/or minima which reflect the change of drifting and rotational direction. Those are corresponding to the results of time variation of orientation of the pca seen in Fig. 7 where the orientation angles of the pca are estimated for each of 5-day bin of entire current record. Interesting patterns are evidently found that through the sequences, rotational axes are alternating between clockwise and counter-clockwise with varying the magnitudes of semi-major axis in Fig. 7. The result is a consequence of the spectral components of 13.6 (day) in Fig. 5c.

Magnitudes of semi-major axes for the residual current and wind are also of interest and can be compared each other, as seen in Fig. 8. The straight line best fitted to the magnitude of the major axes shows the slope of 0.03 with correlation coefficient of 0.92. Interestingly, the slope of the fitted line implies the validity of 3 % rule of wind induced drift current. In Fig. 8, median value of 50 (cm/sec) wind speed corresponds approximately to the 1.45 (cm/sec)

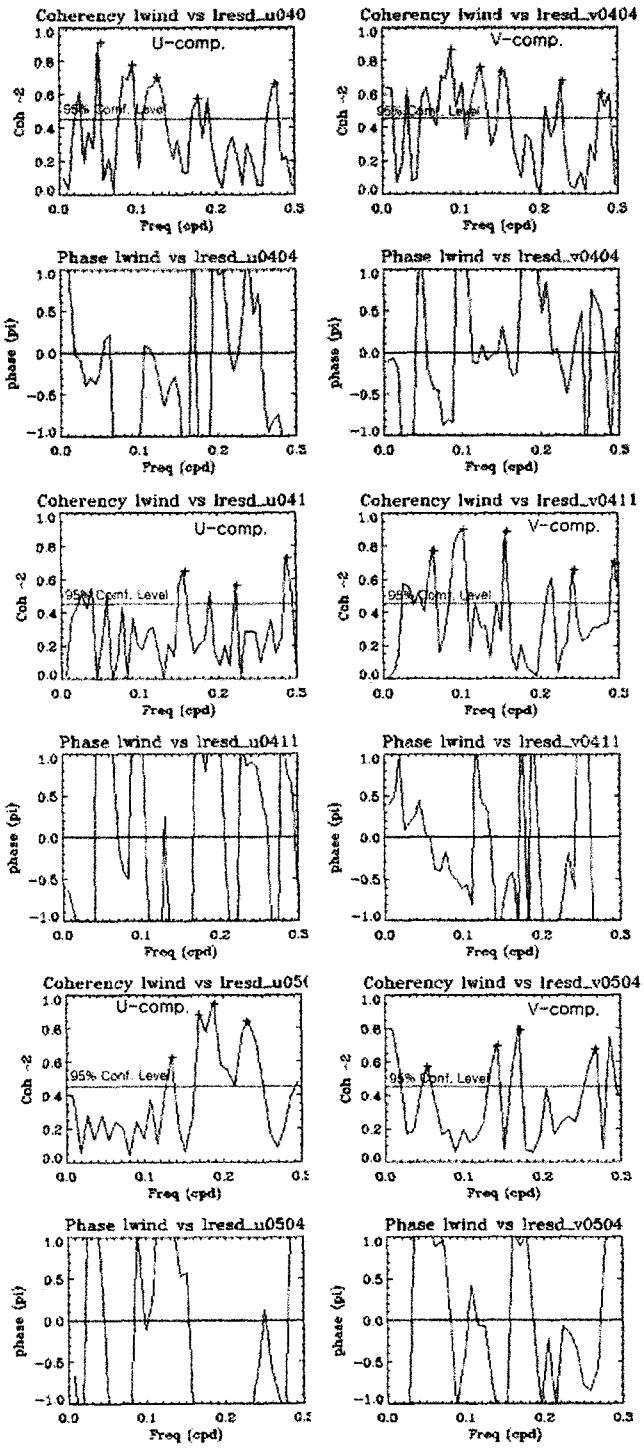

Fig. 9. Coherency between the band-passed current and wind records #2, 3, and 4.

residual current

In the frequency domain, auto- and cross-spectra, coherency and phase between wind and residual current records were estimated for the Records #2, 3 and 4. Here, only

the results of coherency and phase plots are shown in Fig. 9. Several significant coherencies well above 95 % confidence level could be resolved in that 3~5 periodicities ranging from 3.5 to 20.8 (days) were found to be important for each record. Specifically, in the Record #2, period of 8.3 (day) is common for both u- and v-components of wind and residual current and highest coherency peak occurred at 20.8 (day) for u-comp with 1.2-day phase lag of wind to current. In the Record #3, period of 6.6 (day) is common for both u- and v-components of wind and residual current and highest coherency peak occurred at 10.2 (day) for v-comp with 2.6-day phase lead of wind to current. In the Record #4, period of 6.1 (day) is common for both u- and v-components of wind and residual current and highest coherency peak occurred at 5.4 (day) for u-comp with 2.7-day phase lead of wind to current.

The influence of the Nam-Gang Dam water discharge on the residual current

The Nam-Gang Dam water was discharged into the Kangjin Bay through the Sachon Bay, starting to release at 23:37 on August 18th, 2004 and to finish at 11:37 on Aug. 30th, 2004. The duration of water discharge was 12-day and 12-hour with the total volume amount of 830,176,000 (m^3). The peak discharge rate was 3523 (cms) at 01:38 on Aug. 19th. The fresh water release had tremendous impact on the hydrodynamics and hydrography of the KB and led to the catastrophic episode of mass mortality of the large-arc shell being cultured in the KB. The impact could be shown by the abrupt drop of temperature and salinity shown in Fig. 10. Local salinity in the KB was diluted to be 10.63 (psu), comparing to normal salinity of 31.9 (psu) with drop of more than 20 (psu). Southward

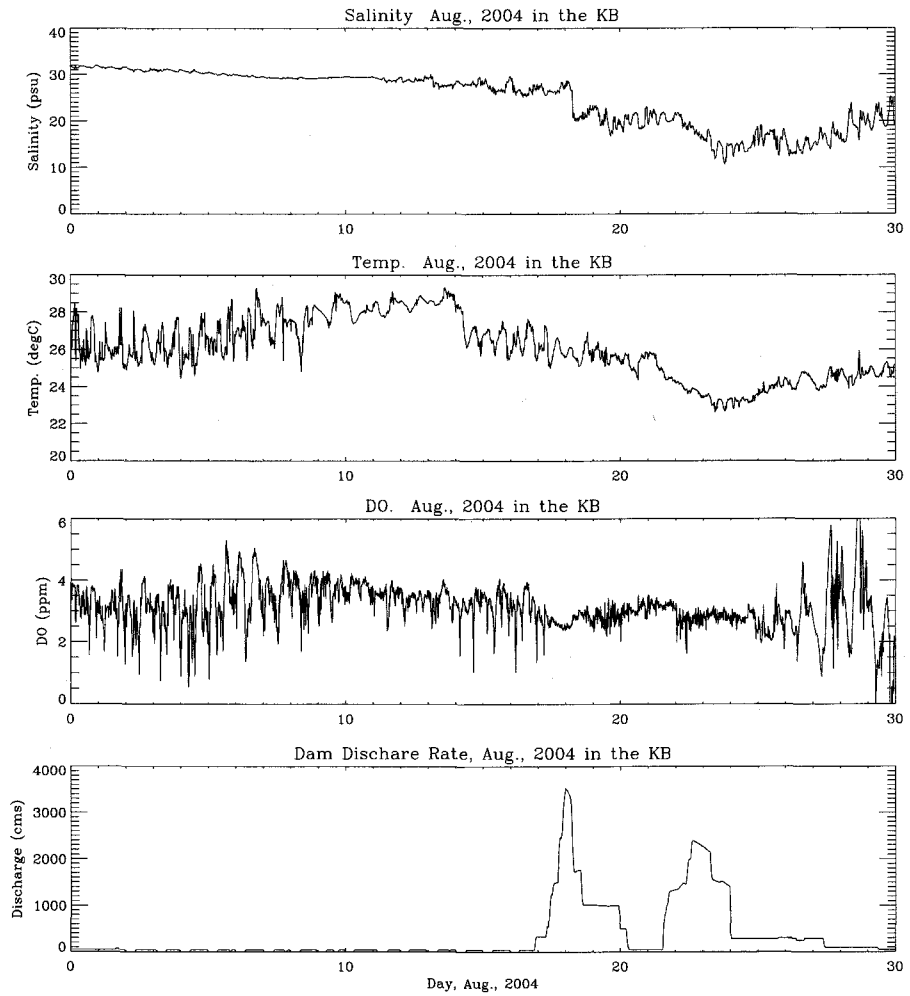

Fig. 10. Time series of salinity, temperature, dissolved oxygen and dam water discharge rate for the period of Aug., 1st to 30th, 2004. Observation depth of salinity, temperature and D.O. is 50 cm above bottom at the real-time monitoring station 1 (Fig. 1).

current speed during water discharge reached 32.6 (cm/sec) of which residual component is estimated to be 7.09 (cm/sec) in Table 4. Owing to the buoyancy of the fresh water in the upper layer, strong stratification was developed so that density-driven current was directed toward open ocean (in this case, southward). This situation casts an important and significant challenge to the study of coastal plume dynamics and its impact on the local fishery. Separate numerical modeling works were carried out and readers interested in more detail may refer to Ro et al. (2005) and Ro (2007).

5. Summary and Discussion

This study analyzed the 5 current meter records spanning from March 22, 2004 to Nov. 6, 2005 in the Kangjin Bay, South Sea, Korea. The database of long records over 500 (day) provides us with a very rare opportunity to understand the tidal current characteristics and its monthly variation particularly in the coastal embayment area such as the Kangjin Bay.

The results of harmonic analyses of the current records show that it is very much of semi-diurnal type with form number of 0.12 and almost rectilinear with orientation of the major axis toward northeast. The semi-major and -minor axes range from 12.35 to 17.5 (cm/sec) and 0.07 to 0.95 (cm/sec) for M2 harmonics, while S2 harmonics range from 6.3 to 9.72 (cm/sec) and 0.09 to 0.52 (cm/sec), respectively. Average ratio of S2 to M2 semi-major axis is 0.53, while average ratio of O1 to K1 semi-major axis is 0.45. The harmonics of tidal current components show variability more severely than the tidal heights since non-linearity plays a bigger role in tidal current than in tidal elevation in general.

In the spectral analysis of residual current, significant spectral peaks could be resolved which lie on the folding frequencies of 1/30 (cpd) in most of records. Among many spectral components, the period of 13.6-day is found to be important for the Record #4 which is attributed to the variation of the principal axis and its orientation angle as well as rotational axis. The influence of the local wind on the residual current is investigated in two ways. First, the progressive vector diagrams of band-passed residual current and wind were compared to each other to find the influences of wind on current in terms of net drift. Interestingly, two types of behaviors are obvious that one is unidirectional drift and the other is rotational motion. Secondly, the progressive vector diagram for the Record #4 is associated with the spectral components of 13.6 (day), which show alternating rotations between clockwise and counter-clockwise axis. Another interesting finding is that by the correlation of the semi-major of wind and residual current, 3 % rule holds true approximately to drive 1.45 (cm/sec) drift current by 0.5 (m/sec) wind speed.

The implications of the net drift of the residual current in the coastal embayment system are manifold. One is that it would have a significant impact on the survival rate of the fish eggs and/or shell larvae in the early life cycle. It is especially true in the KB, since it is well known for aqua-culturing beds for the renowned large-arc shell (*Scapharca Broughtonii*). With regard to this aspect, more study is required in the near future. The other impact can be speculated that the net drift will deposit the pollutant and waste material introduced through the Noryang Channel and Sachon Bay onto particular areas, most probably near the southwestern part of the KB. This factor should be considered in managing the water and sediment quality in the Kangjin Bay.

The analysis of the tidal current records in the KB can not be complete without other supporting tools of understanding the local complicated current dynamics. In addition to this study, a parallel study is being made by using high-resolution 3-D numerical modeling approach and is to be published in a separate paper (Ro 2007). Both studies are complimentary to each other, and hope to extend our level of understanding the coastal dynamics of the South Sea, Korea.

Acknowledgement

This study (MNF 22003011-3-2-SB010) was funded by the MOMAF administered by Korea Institute of Marine Science & Technology Promotion. The publication of this study is partly supported by the Chungnam National University Research Fund during the author's sabbatical leave to Ohio State University in 2006-2007. The author appreciates the reviewers' comments and editorial corrections.

References

Blackman, R.B. and J.W. Tukey. 1958. The Measurement Of Power Spectra from the Point of View of Communication

Engineering. Dover Publications. 190 p.

Cai S., Q. Huang, and X. Long. 2003. Three-dimensional numerical model study of the residual current in the South China Sea. *Oceanol. Acta,* **26**(5), 597-607.

Chang, S.D., C.K. Kim, and J.S. Lee. 1993. Field observations and hydraulic model experiments of tidal currents in Chinhae Bay. *J. Korean Fish. Soc.*, **26**(4), 346-352.

Cho, H.Y., J.W. Chae, and S.Y. Chun. 2002. Stratification and do concentration changes in Chinhae-Masan Bay. *J. Korean Soc. Coast. Ocean Eng.,* **14**(4), 295-307.

Cho, K.D., C.I. Cho, B.G. Lee, K.W. Cho, and D.S. Kim. 1993. Study on the water and material exchange in Deukryang Bay I. Volume transport and turnover time of sea water. *J. Environ. Sci.,* **7**(3), 311-319.

Duchon, C.E. 1979. Lanczos filtering in one and two dimensions. *J. Appl. Met.,* **18**, 1016-1022.

Emery, W.J. and R.E. Thomson. 2001. Data Analysis Methods in Physical Oceanography. Elsevier. 638 p.

Foreman, M.G.G. 1978. Manual for tidal current analysis and prediction. Pacific Marine Science Report 78-6. Institute of Ocean Sciences, Patricia Bay, Victoria, B.C. 39 p.

Foreman, M.G.G., D.J. Stucchi, Y. Zhang, and A.M. Baptista. 2006. Estuarine and tidal currents in the Broughton Archipelago. *Atmos. Ocean*, **44**(1), 47-63.

Guo, X. and T. Yanagi. 1996. Seasonal variation of residual current in Tokyo Bay, Japan-diagnostic numerical experiments. *J. Oceanogr.*, **52**, 597-616.

Jenkins, G.M. and D.G. Watts. 1968. Spectral Analysis and Its Applications. Holden-Day. 525 p.

Han, M.W., K.I. Chang, and Y.C. Park. 2001. Distribution and hydrodynamic model of the *Keumdong* oil spill in Kwangyang Bay, Korea. *Environ. Int.,* **26**(7-8), 457-463.

Kashiwai, M. 1984. Tidal residual circulation produced by a tidal vortex. Part 1. Life-history of a tidal vortex. *J. Oceanogr. Soc. Japan,* **40**(6), 279-294.

Lee, D.I., C.K. Park, and H.S. Cho. 2005. Ecological modeling for water quality management of Kwangyang Bay, Korea. *J. Environ. Manage.,* **74**(4), 327-337.

Lee, J.C., J.C. Kim, and M.W. Park. 2006. Currents in the northeastern Gwangyang Bay. *J. Korean Soc. Oceanogr.,* **11**(4), 172-178.

Liu, J.T. 1992. The influence of episodic weather events on tidal residual currents: A case study at Sebastian Inlet, Florida. *Estuaries*, **15**(2), 109-121.

Marinone, S.G. and M.F. Lavýn. 2005. Tidal current ellipses in a three-dimensional baroclinic numerical model of the Gulf of California. *Estuar. Coast. Shelf Sci.,* **64**, 519-530.

Ou, H.W., R.C. Beardsley, D. Meyer, W.C. Boicourt, and B. Butman. 1980. An analysis of subtidal current fluctuations in the Middle Atlantic Bight. *J. Phys. Oceanogr.*, **11**(10), 1383-1392.

Park, K., H.S. Jung, H.S. Kim, and S.M. Ahn. 2005. Three-dimensional hydrodynamic-eutrophication model (HEM-3D): Application to Kwang-Yang Bay, Korea. *Mar. Environ. Res.,* **60**(2), 171-193.

Pawlowicz, R., B. Beardsley, and S. Lentz. 2002. Classical tidal harmonic analysis including error estimates in MATLAB using T_TIDE. *Comput. Geosci.,* **28**, 929-937.

Ro, Y.J., W.S. Jun, K.Y. Jung, and B.H. Kim. 2005. Numerical modeling of river plume in the Kangjin Bay and its implication for the ecosystem. Proc. Autumn Meeting, 2005 Korean Soc. Oceanogr., p. 218-220.

Ro, Y.J. 2006. Internet-based realtime monitoring of the environmental parameters in the marine large-arc shell culture bed and its productivity assessment model. Final Report, Ministry of Marine and Fishery. 155 p.

Ro, Y.J. 2007. 3-D baroclinic numerical modeling of the tidal and density current in the Kangjin Bay, South Sea, Korea, Part I: Tide and tidal current. *J. Korean Soc. Coast. Ocean Eng.* (In Press)

Yanagi, T. 1983. Generation mechanisms of tidal residual circulation. *J. Oceanogr. Soc. Japan,* **39**(4), 156-166.

Yasuda H. 1980. Generating mechanism of the tidal residual current due to the coastal boundary layer. *J. Oceanogr. Soc. Japan,* **35**(6), 241-252.

Wang S.Y. and M.X. Tang. 2004. Exact Confidence Interval for Magnitude-Squared Coherence Estimates. *IEEE Signal. Proc. Lett.,* **11**(3), 326-329.

Wong, K.C. 1998. The seasonal and subtidal variability in the source region of the Delaware Coastal Current. *Estuar. Coast. Shelf Sci.,* **47**, 1-19.

Valle-Levinson, A. and T. Matsuno. 2003. Tidal and subtidal flow along a cross-shelf transect on the East China Sea. *J. Oceanogr.*, **59**, 573-584.